Front. Electr. Electron. Eng. China 2009, 4(1): 93–97
DOI 10.1007/s11460-008-0081-8

RESEARCH ARTICLE

Cihui LIU, Ran YAO, Jianfeng SU, Zeyu MA, Zhuxi FU

Luminescence and recombine centre in ZnO/Si films

© Higher Education Press and Springer-Verlag 2008

Abstract The D^0h luminescence of ZnO films deposited on p-type Si substrates is produced by metal-organic chemical vapor deposition (MOCVD). After annealing in the air at 700°C for an hour, the photoluminescence (PL) spectra, the *I*-*V* characteristics and the deep level transient spectroscopy (DLTS) of the samples are measured. All the samples have a rectification characteristic. DLTS signals show two deep levels of E_1 and E_2. The Gaussian fit curves of the PL spectra at room temperature show three luminescence lines *b*, *c* and *d*, of which *b* is attributed to the exciton emission. The donor level E_1 measured by DLTS and the location state donor ionization energy E_d of the closely neighboring emission lines *c* and *d* are correlated. E_1 is judged as neutral donor bound to hole emission (D^0h). Moreover, the intensity of the PL spectra decreases while the relative density of E_2 increases, showing that E_2 has the property of a non-radiative center.

Keywords metal-organic chemical vapor deposition (MOCVD), ZnO/p-Si, heterojunction, defect

1 Introduction

Short wave photoelectron materials have been intensively studied in recent years because they can increase record density of optical communications and information.

Although the wide-gap semiconductor material ZnO has been explored for dozens of years with broad applications in many fields [1–8], the luminescence property of ZnO has not drawn much attention until 1996, when the phenomena of microcrystalline structure of ZnO films optically pumped ultraviolet stimulated emission was reported [9].

The deep levels in semi-conductors forbidden band are important in light emitting devices. Electrons transit from conduction bands to valence bands and emit photons. The existing deep levels will decrease the luminance efficiency, while the radiative recombination of some deep levels will increase luminance efficiency [10]. Therefore, it is important to understand the luminance mechanism of ZnO films.

The research shows that the optical and electricity properties of ZnO films vary greatly under different preparing conditions. Metal-organic chemical vapor deposition (MOCVD) has advantages as a preparing method such as lower growth temperature, easier growth control and higher quality prepared films [11]. In this article, we study optical and electricity properties of the ZnO/p-Si structure prepared by MOCVD through deep level transient spectroscopy (DLTS), *I*-*V* characteristic, PL spectrum measurement results, and discuss the property of deep level centers E_1 and E_2.

2 Experiments

Undoped ZnO films were produced in a vertical MOCVD system designed and built by the authors. Diethylzinc (DEZ) and carbon dioxide (CO_2), with a purity of 99.999%, are used as precursors to the growth of ZnO films. Pure nitrogen which was used as carrier gas with rates of 0.86, 1.4, and 1.7 slm respectively was shunted in two ways into the ZnO reactor. On one hand, the carrier gas passed through the DEZ bubbler at a flow rate of 10 sccm; on the other hand, the carrier gas was connected to the exit of the bubbler with a flow rate controlled at 50 sccm to accelerate the transportation of DEZ to the reactor. The temperature of the bubbler was kept at 10°C during ZnO growth and the growth temperature was 600°C. The flux of CO_2 is 80 sccm. The film was deposited on the surface of p-Si (100). The pressure in the ZnO reactor was 133.3 Pa, and the well-grown films were annealed in the air at 700°C for an hour.

A 0.001 Hz ultralow frequency sawtooth wave generator (model 439 function generator) was used as the voltage source for *I*-*V* measurement. During measurement, the samples were kept in a dark chamber. More experimental details can be found in Ref. [12]. DLTS measurements were performed within 77–350 K temper-

Translated from *Chinese Journal of Semiconductors*, 2007, 28(2): 196–199 [译自: 半导体学报]

Cihui LIU (✉), Ran YAO, Jianfeng SU, Zeyu MA, Zhuxi FU
Department of Physics, University of Science and Technology of China, Hefei 230026, China
E-mail: chliu@ustc.edu.cn

ature range using NJ. M. DLTS set. The PL spectra were measured with a model 850 fluorescence spectrometer at room temperature, and the excited wavelength is 210 nm. The double-crystal *X*-ray diffraction (XRD) patterns of all the samples were measured by a Philips *X*'Pert Diffractometer with a symmetrical Ge (220) monochromator.

3 Results and discussion

Figure 1 shows the XRD patterns of ZnO/Si films prepared by MOCVD, with the total flux of N_2 at 0.86, 1.4 and 1.7 slm. As seen from Fig. 1, all the samples have a good orientation in the *c* axis. The half bandwidth of ZnO (002) diffraction peaks and intensity increase largely when the carrier gas flow rate increases.

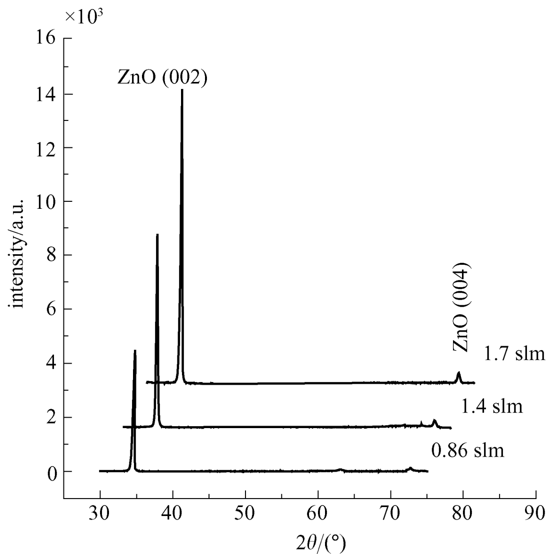

Fig. 1 XRD patterns of ZnO films grown with different flow rates of N_2 eluting gas

Figure 2 shows the *I-V* characteristic of the sample S2a (the carrier gas flow rate is 1.4 slm). The curve is shifted to voltage axis when the forward bias voltage is above 1.5 V. The curve is basically linear under 1.5 V, which can be explained as a result that the current increases exponentially to voltage. The forward current is nearly milliampere in magnitude, with a large reverse leakage current. Carbon contamination in the prepared process by MOCVD may increase reverse leakage current. The voltage-current characteristic of the samples can be depicted by [13]

$$I_F = I_0 \exp\left(\frac{qV_F}{nkT}\right), \tag{1}$$

$$I_0 = A^* ST^2 \exp\left(\frac{-q\phi_B}{KT}\right). \tag{2}$$

In Eq. (1), I_0 is the saturation reverse leakage current of the heterogeneous junction; V_F is the bias voltage on p

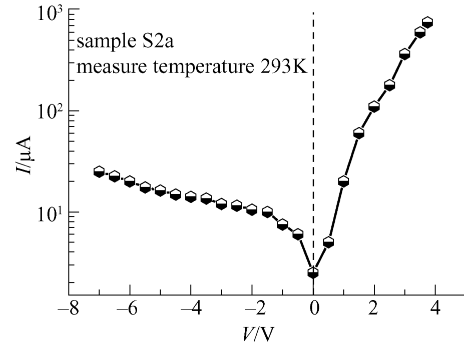

Fig. 2 *I-V* characteristic of ZnO/Si heterojunction

and n type semiconductor; *n* is the ideality factor; *k* is the Boltzmann constant; *T* is the Kelvin temperature; A^* is the effective Richardson constant; *S* is the effective section areas of heterogeneous junction; and ϕ_B is the potential barrier height of the heterogeneous junction. Fitting the forward *I-V* curve in Fig. 2 using the relationship $\ln I_F - qV_F/nkT$ and setting 1.5 V as the division point, we obtain $V_F \leqslant 1.5$ V, $n \leqslant 16$ and $V_F \geqslant 1.5$ V, $n \leqslant 35$ respectively. The ideality factors of the samples deviate significantly from that of the ideal case, showing that a higher series bulk resistance in heterogeneous junction exists. Considering the series bulk resistance influence on the transport process, Eq. (1) can be modified as

$$V_F = \frac{kT}{q} \ln\left(\frac{I_F}{A^* T^2}\right) + \phi_B + I_F R_{on}. \tag{3}$$

In Eq. (3), the first and the second items are voltage drop on the ideal heterogeneous junction; R_{on} is forward bulk resistance; and $I_F R_{on}$ is the voltage drop of heat emission current on bulk resistance. The voltage dropped on bulk resistance R_{on} increases rapidly when I_F rises, but the bias voltage drops on heterogeneous junction increase slightly. This shows that the ideal factor becomes larger when the bias voltage is high. The ZnO/Si structure has an intrinsic property of higher bulk resistance, which is relative to the low charge mobility in ZnO films [14]. Furthermore, different temperatures of *I-V* measurement and the surface state under different bias voltages can greatly affect the barrier, which then influences the ideal factor.

Figure 3 is the DLTS spectrum of the sample S2a. Based on the DLTS theory, the electron emission rate e_n can be expressed as [15]

$$e_n = B_n T^2 \exp\left(-\frac{E_C - E_T}{kT_P}\right). \tag{4}$$

In Eq. (4), the constant B_n has no relation with the temperature; $E_C - E_T$ is the distance of deep levels between the forbidden band and conduction band; and T_P is the deep level emission peak temperature. As shown in DLTS spectra in Fig. 3, there are two deep level emission peaks in 136.1 K and 238 K, where the former is E_1

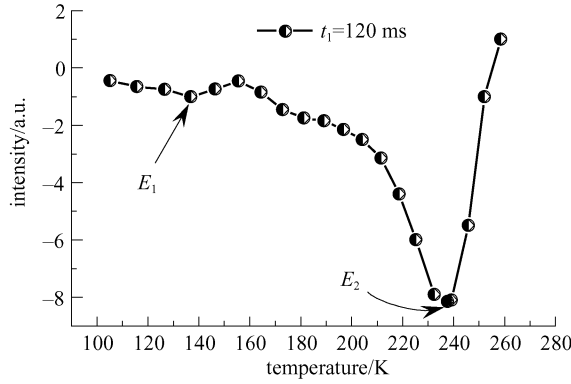

Fig. 3 Typical DLTS temperature spectrum of sample S2a

and the latter is E_2. The DLTS measurement can obtain the relationship between the deep level electron emission rate and the emission peak temperature of T_P by changing the sample rate window t_1. Fitting the curve by $\ln(e_n/T^2) - 1/T$ using Eq. (4) obtains the location of the deep level by slope. By the principle of DLTS measurement, the relative gap state density of the deep level has a relationship with the altitude of the DLTS spectrum peak. We can then obtain the relative gap state density of the deep level using the above method. The samples grow under three different carrier gas rates, of which all have the deep levels E_1 and E_2. However, the relative gap state density and the location of deep level centers are slightly different as shown in Table 1. In Table 1, N_t is the deep level gap state density, N_B is the carrier concentration of ZnO films and N_t/N_B is the relative gap state density of the deep level.

Table 1 Characteristics of deep levels at various preparation fluxes in samples

sample	carrier gas flux/slm	energy level/eV	N_t/N_B
S2p	0.86	$E_1 = E_C - 0.15 \pm 0.60$	1.34%
		$E_2 = E_C - 0.47 \pm 0.07$	3.39%
S2a	1.4	$E_1 = E_C - 0.13 \pm 0.02$	1.01%
		$E_2 = E_C - 0.43 \pm 0.05$	5.10%
S1p	1.7	$E_1 = E_C - 0.09 \pm 0.06$	1.99%
		$E_2 = E_C - 0.41 \pm 0.07$	8.71%

Figure 4 shows the PL spectrum of sample S2a (curve *a*). The asymmetry of PL spectrum reveals that the luminescence energy of the spectrum is not single. By Gaussian fitting the PL spectrum, we can obtain ultraviolet emitting lines which have a luminescence energy of 3.242 eV (curve *d*), 3.250 eV (curve *c*) and 3.305 eV (curve *b*) respectively. As ZnO has 60 meV exciton bound energy at room temperature, we consider that the emitting line *b* at 3.305 eV is the exciton emission in ZnO. The emitting lines *c* and *d* are located on the lower energy position of the exciton emission line *b*. The position of the emission lines *c* and *d* should be located in the forbidden band of the semiconductor, and the position can be obtained by [16]

$$E_{\text{emission}} = E_g - E_d + \frac{kT}{2}. \quad (5)$$

In Eq. (5), E_{emission} is the energy of light emission; E_g is the width of the forbidden band; and E_d is the donor ionization energy. Taking the emitting energy of the luminescence line *c* of 3.250 eV in Fig. 4 and using it in Eq. (5), we get the ionization energy $E_d = 0.1333$ eV. The location of the luminescence line *c* is $E_C - 0.1333$ eV in the forbidden band, which coincides with the donor deep level $E_1 = E_C - (0.13 \text{ eV} \pm 0.02)$ detected in the sample of S2a by DLTS. Thus, it can be deduced that the donor deep level E_1 is the local state radiation center. According to the location of E_1 in the forbidden band, the electron transition of E_1 level coincides with the composite luminescent characteristic of D^0h. Since the luminescence line *c* is very close to the energy line *d*, the DLTS measurement also cannot tell the difference between the two luminescence centers. The deep level center E_1 is probably composed of the emission with closed energy.

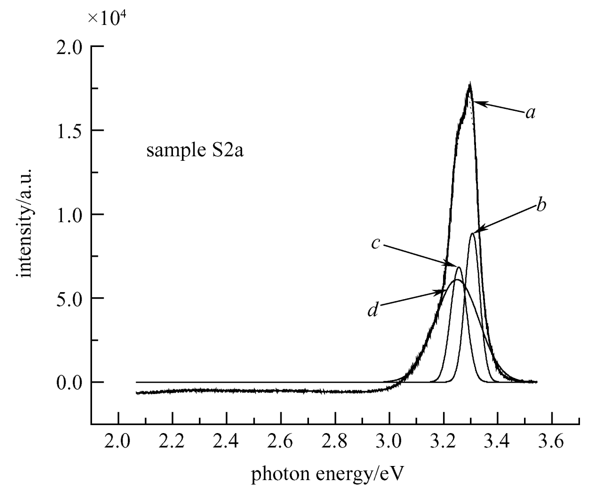

Fig. 4 PL spectrum(curve *a*) of ZnO/p-Si film deposited by MOCVD and Gaussian fit spectra (curves *b*, *c* and *d*)

Figure 5 shows that the room temperature PL spectra of ZnO films with ZnO/p-Si structure are grown under three different carrier gas rates. The samples S1p and S2a have an exciton luminescence peak of 376.3 nm. The sample S2p has an exciton luminescence peak of 377.3 nm. There is an obvious shoulder at 382 nm in the PL spectrum of samples grown under the 1.4 and 1.7 slm carrier gas rates respectively (the dashed line in Fig. 5), and the energy of the luminescence line is about 3.246 eV. Although the luminescence line of the sample S2p that grows under 0.86 slm has no obviously heaved shoulder, the asymmetry of the PL spectrum can be clearly observed. We can also observe the influence of the increased carrier gas on the PL spectrum. The location of E_1 becomes shallower, while the carrier gas rate becomes higher as shown in Table 1, which indicates that the local state energy level E_1 has a

relationship with the rate of carrier gas. It is established that different carrier gas rates not only influence the best orientation degree of crystal nucleus and grain size, but also change grain boundary and surface roughness. The energy state near the band edge is highly sensitive to crystal structure defects [17], and the variant of film structure influences the binding state of the local state directly. The correlation between the state of deep level E_1 and the growth carrier gas rates shows that E_1 has a characteristic of structure defect emission.

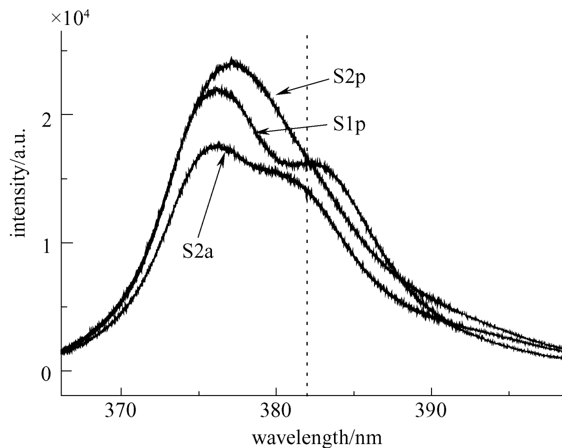

Fig. 5 PL spectra of samples S2p, S2a, and S1p at room temperature

The deep level E_2 detected by DLTS in the samples is shown in Table 1. First, it has a higher relative gap density. Second, the location of E_2 becomes shallower while the carrier gas rates are higher. There are no obvious emitting lines related to the energy E_2 in the PL spectrum in Fig. 4. From the E_2 level in the different samples in Table 1, the higher relative gap density, the lower PL spectrum peaks intensity in Fig. 5. This reveals that E_2 level is a recombination center which can influence luminescence intensity.

Experiments show that when the carrier gas rate rises, thin film material deposited on the substrate will increase. The increment of film deposition rate facilitates thicker film growth. The film attempts to restore the inherent crystal lattice constant when its thickness reaches a certain degree. The crystal lattice deformation energy in the film near the substrate will increase, and larger crystal lattice deformation energy will result in dislocation near the substrate. Meanwhile, the mismatch stress between the film and the substrate will decrease. The E_2 level in the samples has properties described above, which reveals that it has a relationship with the deep level center related to internal stress defects.

4 Conclusions

The sample with ZnO/p-Si structure is prepared by MOCVD, which is measured by PL spectrum, *I-V* and DLTS. The experiment reveals the existence of excitons and a neutral donor - valence band (D^0h) luminescence center. The deep level centers E_1 and E_2 detected by the DLTS spectrum are the luminescence and recombination center respectively. The existence of E_2 level affects luminescence intensity.

Acknowledgements This work was supported by the National Natural Science Foundation of China (Grant Nos. 50472009, 10474091) and the Knowledge Innovation Engineering of the Chinese Academy of Sciences (kjcx2-sw-04-02).

References

1. van de pol F C M, Blom F R, Popma T J A. RF planar magnetron sputtered ZnO films I: structural properties. Thin Solid Films, 1991, 204: 349–364
2. Gorla C R, Emanetoglu N W, Liang S, et al. Structural, optical, and surface acoustic wave properties of epitaxial ZnO films grown on ($01\bar{1}2$) sapphire by metalorganic chemical vapor deposition . Journal of Applied Physics, 1999, 85(5): 2595–2602
3. Gao P, Wang Z. Nanoarchitectures of semiconducting and piezoelectric zinc oxide. Journal of Applied Physics, 2005, 97(4): 044304
4. Chen Z Q, Kawasuso A, Xu Y, et al. Production and recovery of defects in phosphorus-implanted ZnO. Journal of Applied Physics, 2005, 97(1): 013528
5. Hur T B, Hwang Y H, Kim H K, et al. Strain effects in ZnO thin films and nanoparticles. Journal of Applied Physics, 2006, 99(6): 064308
6. Vayssieres L, Keis K, Hagfeldt A, et al. Three-dimensional array of highly oriented crystalline ZnO microtubes. Chemistry of Materials, 2001, 13(12): 4395–4398
7. Chu T L, Chu S S. Thin film II–VI photovoltaics. Solid-State Electronics, 1995, 38(3): 533–549
8. Keis K, Magnusson E, Lindstrom H, et al. A 5% efficient photoelectrochemical solar cell based on nanostructured ZnO electrodes. Solar Energy Materials and Solar Cells, 2002, 73(1): 51–58
9. Yu P, Tang Z K, Wong G K L, et al. Room temperature stimulated emission from ZnO quantum dot films. In: Proceedings of the 23rd International Conference on the Physics of Semiconductors. Singapore: World Scientific, 1996, 2: 1453–1456
10. Liu C H, Zhu J J, Lin B X, et al. Deep level of ZnO/p-Si heterostructure and its influence on the photoluminescence. Chinese Journal of Luminescence, 2001, 22(3): 218–222 (in Chinese)
11. Chen Z M, Wang J L. Basic material physics for semiconductor devices. Beijing: Science Press, 1999: 49–50 (in Chinese)
12. Liu C H, Chen Y L, Lin B X, et al. Electrical properties of ZnO/Si heterostructure. Chinese Physics Letters, 2001, 18(8): 1108–1110
13. Sze S M. Physics of Semiconductor Devices. New York: Wiley, 1981, 255–265
14. Nikitin S E, Nikolaev Y A, Polushina I K, et al. Photoelectric phenomena in ZnO: Al-p-Si heterostructures. Semiconductors, 2003, 37(11): 1291–1295
15. Park W I, Yi G C. Photoluminescent properties of ZnO thin films grown on SiO_2/Si (100) by metal-organic chemical vapor deposition. Journal of Electronic Materials, 2001, 30(10): L32–L35

16. Tamura K, Makino T, Tsukazaki A, et al. Donor-acceptor pair luminescence in nitrogen-doped ZnO films grown on lattice-matched $ScAlMgO_4$ (0001) substrates. Solid State Communications, 2003, 127(4): 265–269

17. Baltrameyunas R, Gavryushin V, Rachyukaitis G, et al. Effects of deformation of the fundamental edge by defects on two-photon spectroscopy of semiconductors. Soviet Physics-Solid State, 1991, 33(3): 537–538